# Differential-driven thin-film lithium niobate micro-ring modulator

1st Jiacheng Liu
*State Key Laboratory of Advanced Optical Communication Systems and Networks*
*Shanghai Jiao Tong University*
Shanghai 200240, China
jiacheng.liu@sjtu.edu.cn

2nd Jiangbing Du*
*State Key Laboratory of Advanced Optical Communication Systems and Networks*
*Shanghai Jiao Tong University*
Shanghai 200240, China
*Peng Cheng Laboratory*
Shenzhen 518055, China
dujiangbing@sjtu.edu.cn

3rd Wenjia Zhang
*State Key Laboratory of Advanced Optical Communication Systems and Networks*
*Shanghai Jiao Tong University*
Shanghai 200240, China
*Peng Cheng Laboratory*
Shenzhen 518055, China
wenjia.zhang@sjtu.edu.cn

4th Zuyuan He
*State Key Laboratory of Advanced Optical Communication Systems and Networks*
*Shanghai Jiao Tong University*
Shanghai 200240, China
*Peng Cheng Laboratory*
Shenzhen 518055, China
zuyuanhe@sjtu.edu.cn

***Abstract*—Differential-driven thin-film lithium niobate micro-ring modulator is demonstrated. Two segments of electrode are employed to provide reversed electric field. The fabricated device features a tunability of 1.67 pm/V, supporting data rates up to 20 Gb/s.**

***Index Terms*—Electro-optic modulators, Thin-film lithium niobate, Micro-ring modulators.**

## I. Introduction

Electro-optic (EO) modulator is a key building block required in various applications, such as optical interconnect [1], optical sensing [2], microwave photonics [3] and so on. As the best-known EO material, lithium niobate (LN) has been widely used in commercial EO modulator products owing to its attractive material properties of wide transparent wavelength window, ultra-low optical loss and linear electro-optic modulation effect (Pockels effect) [4]. Recently, with the development of the thin-film lithium niobate (TFLN) nanofabrication technology, various TFLN modulators with shrunk footprint and high EO modulation bandwidth have been demonstrated. During the past decades, TFLN traveling wave Mach-Zehnder modulator (MZM) with 3-dB bandwidth up to 100 GHz was achieved [5]. The 3-dB bandwidth could be further improved to more than 100 GHz by using capacity loaded traveling-wave electrode on quartz substrate [6]. However, classic TFLN MZM usually features a large footprint of several centimeters due to the limited Pockels coefficient of 30 pm/V [7].

To increase the modulation efficiency of the TFLN modulator, resonant structures can be employed such as micro-ring resonator, photonic crystal cavities and so on. Numerous research on TFLN micro-ring modulator (MRM) have been carried out based on LN rib waveguide [8], full-etched strip waveguide [9] and hybrid $Si_3N_4$-LN waveguide structure [10]. Previous research on LN MRM usually used a single-drive electrode configuration. Differential driving is a more feasible future route because differential driver circuit is widely accessible commercially [11]. Furthermore, differential transmission line pairs feature better RF shielding capacity, which may be benefitial to further reduce the device footprint for large scale integration.

In this work, a differential-driven TFLN MRM, for the first time, to our best of knowledge, was proposed and experimentally demonstrated. Two segments of electrode are employed to provide reversed electric field on a LN ring resonator. Tunability of 1.67 pm/V was obtained and 20 Gb/s OOK modulation was experimentally demonstrated.

## II. Device structure and working principle

Fig. 1(a) shows the schematic structure of the the proposed differential-driven TFLN MRM. Two segments of electrode are employed on the straight part of the racetrack resonator. By ultilizing a differential signal through a GSGSG radio frequency (RF) probe, reversed electric field was loaded on each side of the phase shifter, results in a shift of the resonance

National Key R&D Program of China (2018YFB1801804); The National Natural Science Foundation of China ( 62122047, 61935011); The Major Key Project of PCL (PCL2021A1).

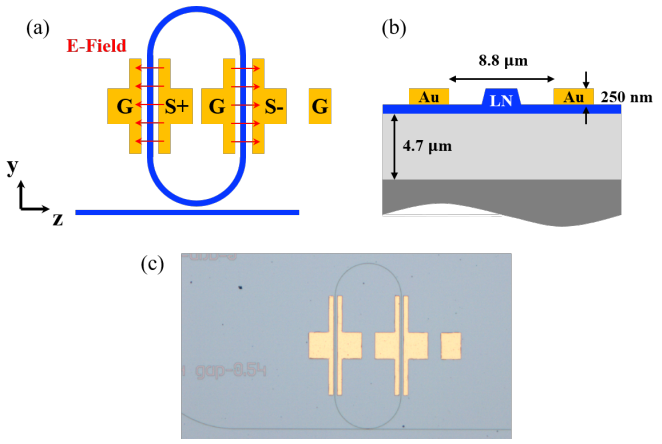


Fig. 1. (a) Schematic structure of the proposed modulator. (b) Cross-section of the modulator. (c) Microscope image of the fabricated modulator.

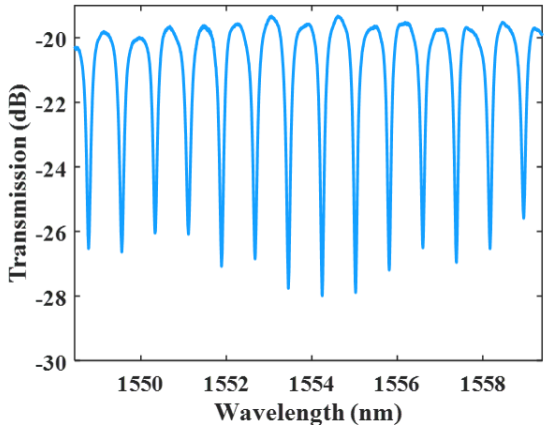


Fig. 2. Measured transmission spectrum of the modulator.

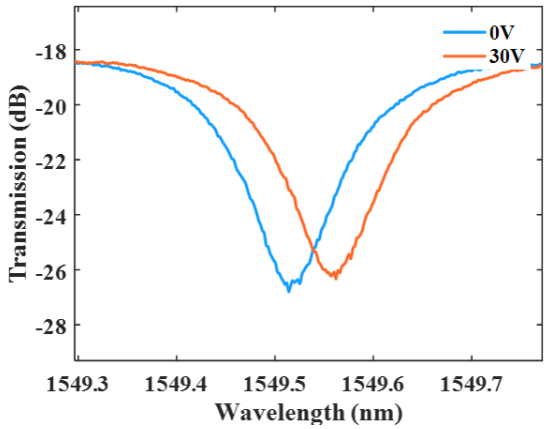


Fig. 3. Transmission spectrum under two different DC bias voltages.

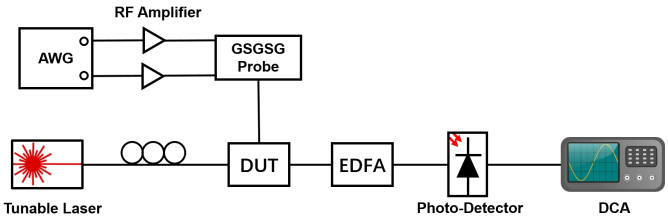


Fig. 4. Experiment setup for high-speed measurement.

wavelength. Fig. 1(b) shows the cross-section of the device. The etched LN rib waveguide width is set to be 800 nm. The waveguide height is 600 nm with a 300-nm slab such that it can support a single transverse-electric (TE) polarized fundamental mode at a wavelength of 1550 nm. The electrode gap is set to be 8.8 $\mu$m due to the limited alignment accuracy of the UV lithography. The electrode length is designed to be 300 $\mu$m. To avoid excessive bending loss, the bending radius of the racetrack is set to 100 $\mu$m. The entire footprint of the device is 200 $\mu$m×500 $\mu$m.

The device was fabricated on an lithium niobate on insulator (LNOI) wafer with 600-nm X-cut LN membrane. The bottom $SiO_2$ cladding is 4.7-$\mu$m thick. The micro-ring structure was patterned by e-beam lithography (EBL) and partly etched by dry-etching process. 250-nm thick Au electrodes were deposited and patterned by lift-off process. The microscope image of the fabricated device is shown in Fig. 1(c).

## III. Device Characterization

The static transmission spectrum of the differential-driven LN MRM was first measured by using a tunable CW laser (Santec TSL-710) and a photodetector. The tunable laser source is coupled to the device under test (DUT) using a lensed fiber, which is aligned to launch TE-polarized light. The measured result is shown in Fig. 2. It can be seen that the overall optical insertion loss of the device is about 20 dB, mainly comes from the unpolished waveguide end face. The MRM has a free spectral range (FSR) of 0.8 nm, with static extinction ratio up to 9 dB. The transmission spectrum under two different bias voltages is shown in Fig. 3. We observed a wavelength shift of 50 pm from 0 V to 30 V DC voltage, corresponding to a tuning efficiency of 1.67 pm/V.

To verify the high-speed performance of the fabricated device, We carried out high-speed data transmission experiment on the proposed modulator. The experiment setup for the high-speed measurement is shown in Fig. 4. The CW laser source is tuned to 1554.94 nm with 13 dBm output power. a $2^7$-1 non-return-to-zero (NRZ) pseudo-random binary sequence (PRBS) signal was generated from a 64-GSa/s arbitrary wave generator (AWG, Keysight, M8192A). Differential signal generated from two inverting ports on the same channel of the AWG was first amplified by two RF amplifiers (SHF807C) to 4 Vpp, and was applied to the modulator via a 40-GHz RF probe with GSGSG configuration. The modulated optical signal was amplified through an erbium-doped optical amplifier (EDFA) to compensate the on chip insertion loss and the signal was detected by a 50-GHz photodetector. The photocurrent signal was sent to a digital communication analyzer (DCA) for eye diagram sampling. The corresponding eye diagram of 10 Gb/s

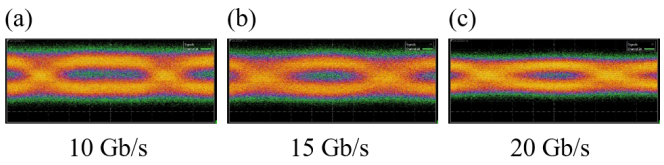


Fig. 5. OOK eye diagram at (a) 10 Gb/s (b) 15 Gb/s and (c) 20 Gb/s data rates.

OOK, 15 Gb/s OOK and 20 Gb/s OOK are shown in Fig. 5 (a), (b) and (c), respectively.

## IV. Conclusion

We proposed and experimentally demonstated a differential-driven TFLN MRM. Two segments of electrode are employed on the straight part of the racetrack resonator to provide reversed electric field. Tuning efficiency of 1.67 pm/V is obtained, and OOK modulation with data rates up to 20 Gb/s was experimentally demonstrated. We believed that this work will pave the way for the development of TFLN modulators with differential-drive configuration.

## References

[1] D. A. B. Miller, "Attojoule optoelectronics for low-energy information processing and communications," *Journal of Lightwave Technology*, vol. 35, no. 3, pp. 346–396, 2017.

[2] M. Soriano-Amat, M. A. Soto, V. Duran, H. F. Martins, S. Martin-Lopez, M. Gonzalez-Herraez, and M. R. Fernández-Ruiz, "Common-path dual-comb spectroscopy using a single electro-optic modulator," *Journal of Lightwave Technology*, vol. 38, no. 18, pp. 5107–5115, 2020.

[3] D. Marpaung, J. Yao, and J. Capmany, "Integrated microwave photonics," *Nature photonics*, vol. 13, no. 2, pp. 80–90, 2019.

[4] P. Ferraro, S. Grilli, and P. De Natale, *Ferroelectric crystals for photonic applications: including nanoscale fabrication and characterization techniques*. Springer, 2009.

[5] C. Wang, M. Zhang, X. Chen, M. Bertrand, A. Shams-Ansari, S. Chandrasekhar, P. Winzer, and M. Lončar, "Integrated lithium niobate electro-optic modulators operating at cmos-compatible voltages," *Nature*, vol. 562, no. 7725, pp. 101–104, 2018.

[6] P. Kharel, C. Reimer, K. Luke, L. He, and M. Zhang, "Breaking voltage–bandwidth limits in integrated lithium niobate modulators using micro-structured electrodes," *Optica*, vol. 8, no. 3, pp. 357–363, Mar 2021.

[7] E. L. Wooten, K. M. Kissa, A. Yi-Yan, E. J. Murphy, D. A. Lafaw, P. F. Hallemeier, D. Maack, D. V. Attanasio, D. J. Fritz, G. J. McBrien *et al.*, "A review of lithium niobate modulators for fiber-optic communications systems," *IEEE Journal of selected topics in Quantum Electronics*, vol. 6, no. 1, pp. 69–82, 2000.

[8] C. Wang, M. Zhang, B. Stern, M. Lipson, and M. Lončar, "Nanophotonic lithium niobate electro-optic modulators," *Opt. Express*, vol. 26, no. 2, pp. 1547–1555, Jan 2018.

[9] M. Bahadori, Y. Yang, A. E. Hassanien, L. L. Goddard, and S. Gong, "Ultra-efficient and fully isotropic monolithic microring modulators in a thin-film lithium niobate photonics platform," *Opt. Express*, vol. 28, no. 20, p. 29644, 2020.

[10] A. N. R. Ahmed, S. Shi, M. Zablocki, P. Yao, and D. W. Prather, "Tunable hybrid silicon nitride and thin-film lithium niobate electro-optic microresonator," *Optics letters*, vol. 44, no. 3, pp. 618–621, 2019.

[11] M. Zhang, C. Wang, P. Kharel, D. Zhu, and M. Lončar, "Integrated lithium niobate electro-optic modulators: when performance meets scalability," *Optica*, vol. 8, no. 5, 2021.